Measuring the Milky Way in M-Dwarfs

Isabel van Vledder
University of Leiden
isamvv@yahoo.com

Dieuwertje van der Vlugt
University of Leiden
dieuwertjevdvlugt@hotmail.com

ABSTRACT

We report 274 M-dwarfs found in the Brightest of Reionizing Galaxies (BoRG) survey for high redshift galaxies. Using these, we fitted a model for the disk and halo with a fixed scale length at h = 2.6 kpc. We found a scale height z_0 of 0.60±0.03 kpc, flattening parameter κ of 0.45±0.04 and a powerlaw-index p of 2.4±0.07. For the total number of M-dwarfs in the disk and halo we found $26.7^{+9.3}_{-6.2} \times 10^9$. The upper limit for the halo fraction of M-dwarfs in the halo is 7^{+5}_{-4} %. The total mass upper limit was determined to be $1.99^{+0.73}_{-0.5} \times 10^9$ M⊙.

Keywords

Galaxy:disk, halo, fundamental parameters, structure-Stars: low-mass

INTRODUCTION

Counting stars has long been used to infer the structure of our Milky Way. This is mostly done with relatively luminous objects due to insufficient data on substellar objects. In our research we will use M-type brown dwarfs found in the Brightest of Reionizing Galaxies (BoRG) survey.

Brown dwarfs are dim substellar objects with masses that range from 13 to 80 Jupiter masses. They lie in between large planets and small stars. Brown dwarfs are not able to fuse hydrogen and thus are not considered stars. Instead, they burn deuterium and lithium. Unlike stars they do not come to their end in a spectacular manner, they just cool down. This is because of the fact that they have a limited amount of nuclear energy due to the exothermic reactions of deuterium and lithium, making them cool over time. Stars can be classified based on their spectra using the letters (in order of decreasing temperature) O B A F G K M. Likewise, brown dwarfs are classified. M-dwarfs are the hottest of their kind followed by L-, T- and Y-dwarfs [1]. These types are divided in subtypes where 0 indicates the hottest and 9 the coolest of a particular type. M0 objects are not classified as brown dwarfs, but as low mass stars. However, because they are dim low mass objects we will still take them into account in this research. Brown dwarfs are believed to be the most numerous luminous objects in galaxies. Studying their distribution can thus tell us a lot about the structure of the Milky Way.

Knowing the number of M-dwarfs is not only useful to study the structure of the Milky Way, but it is also helpful in high redshift galaxy surveys. In images high redshift galaxies and brown dwarfs can appear to have the same colour. One would be able to tell the two apart by their shapes, but with such dim objects achieving high enough quality data to do so proves to be difficult [2]. A good understanding of the initial mass function (IMF) to quantify the contamination of brown dwarfs is needed. The IMF is a distribution of stellar and substellar masses in galaxies when they start to form. From the mass of a star its structure and evolution can be inferred. Likewise, knowing the IMF is a very important step in

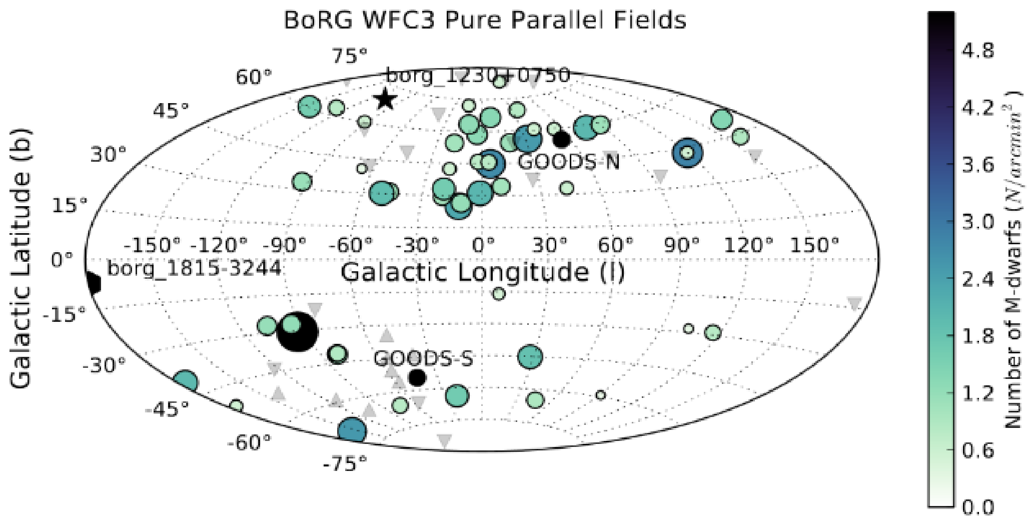

Figure 1 Distribution of BoRG fields and satellite galaxies with the number of M-dwarfs indicated. The fields that are discarded are also indicated; Sagittarius stream field (star) and bulge field (hexagon). The grey triangles indicate the satellite galaxies.

understanding theories on star formation in galaxies. It can be seen as the link between stellar and galactic evolution [3]. The low mass end of the IMF is still mostly unknown. Our research on the number of M-dwarfs may help in determining this part of the IMF. Our main goal however is to find the number of M-dwarfs in our Galaxy and to learn more about its shape. For this we fit a model of the disk, the halo and a combination of the two to the data using a Python implementation of Goodman and Weare's Affine Invariant Markov chain Monte Carlo (MCMC) Ensemble sampler called *emcee* (Foreman-Mackey 2013). We only present the best fitting model.

IDENTIFYING M-DWARFS

The brown dwarfs used in this research were found with the BoRG survey, their distribution is shown in Figure 1.

Observations were made with the Wide Field Camera 3 (WFC3) aboard the Hubble Space Telescope (HST) during a pure parallel program. In this case it means that the WFC3 was on whilst the HST was pointing for primary spectroscopic observations on quasars. The brown dwarfs in the BoRG fields were identified from their morphology and colour. To find the subtypes of the found M-type dwarfs a linear relation between colour and subtype is fitted to spectroscopically identified M-dwarfs. This relation is given below [4].

$$M_{type} = 3.39 \times (V - J) - 3.78$$

Now the distances of the dwarfs can be computed with the distance modulus:

$$Distance = 10^{\frac{m-M}{5}+1}$$

with m the apparent magnitude and M the absolute magnitude. The absolute magnitude is correlated with subtype, this correlation was found by Hawley et al. 2002 [5]. The apparent magnitude is measured. Magnitudes are a measure for the brightness of objects in space.

The model used in this research is a model for a smooth stellar distributions. Substructures like overdensities are not included. To include these structures we need a much more complex model with more parameters. Instead, we exclude fields that contain these kinds of contamination and do the fits with the remaining fields.

MODEL OF DISK AND HALO

The Milky Way Galaxy can be divided into four different components: the bulge, the halo, the thin disk and the thick disk.

The thin and thick disk were believed to be distinct but recent research questions this. It was found that old stars are distributed in disks with a small scale length and a great scale height and that, with decreasing age, the stars are distributed in disks with increasing scale length and decreasing scale height [6][7][8]. In addition to this, a smoothly decreasing function approximately $\sum_R(h) = e^{-h}$ for the surface-mass contributions of stellar populations with scale height h was found [6]. This would not be expected if there was a clear distinction between the thick and the thin disk. Therefore, we assume one model for the disk in this research.

The model that gives the best physical representation of the data is the combination model:

$$\rho(R,z) = \rho_0 e^{-R/h}\,\mathrm{sech}(z/z_0)^2 + \rho_\odot f_h\left(\frac{R^2 + (\frac{z}{\kappa})^2}{{R_\odot}^2 + (\frac{z_\odot}{\kappa})^2}\right)^{\frac{-p}{2}}$$

where $\rho(R,z)$ is the dwarf number density in a point in the disk, ρ_0 the central number density, R the galactocentric radius, h the scale length, z the height above the plane and z_0 the scale height of the disk. ($R_\odot$, $z_\odot$) is the position of the Sun: (8.5 kpc, 0.027 kpc). $\rho_\odot$ the local density, which is the density within a radius of 20 pc of the sun. This was found by Reid et al. 2008 [9]. f_h represents the fraction of stars in the local density that belong to the halo. κ is the flattening parameter and p is the power-law index of the halo. The flattening parameter κ is a measure for the compression of a sphere.

There are two free parameters added in the model: f and δD. f is a parameter which indicates what fraction of the data is bad data adding this gives the most conservative estimates of the parameters. δD is used to get from the measured area density to a volume density.

FIT

For this research we use *emcee* [11], a Python implementation of the Markov chain Monte Carlo (MCMC) Ensemble sampler, to fit the model to the data, with the Metropolis-Hastings method. MCMC provides us with a more efficient way of solving the multidimensional integrals of models with many parameters.

Random samples are drawn from the parameter space and used in the posterior distribution to explore this space. Each chain of samples is called a walker. A quality of emcee [11] is that it sends out an ensemble of walkers, the exact amount set by the user, into parameter space instead of just one. The choice of steps is based on the covariance of the set of walkers. After each step a new posterior probability distribution is evaluated. Steps that increase the posterior probability are accepted and steps that decrease the posterior probability are sometimes accepted based on the ratio of the anterior and new posterior probability [12].

Generally, the walkers will start near the point where maximum probability is believed to be, which can be found by maximizing the likelihood function.

A big advantage of MCMC is that it does not get stuck in local optima and that it can always calculate a 1σ-error even if the distribution is not a Gaussian.

ANALYSIS

To find the best fit values of the parameters and their uncertainties we perform MCMC as described before and because all the M-dwarfs in our dataset are out of the plane (Figure 1), it is difficult to find a constraint on the scale length of the disk. Therefore we take a fixed value for the scale length at 2.6 kpc as was found by Jurić et al. 2008 [10].

We run 500 walkers for 500 steps and use a burn-in period of 50 steps. Burn-in is the term that describes the practice of throwing away some iterations at the beginning of an MCMC run. The burn-in makes sure MCMC has a good

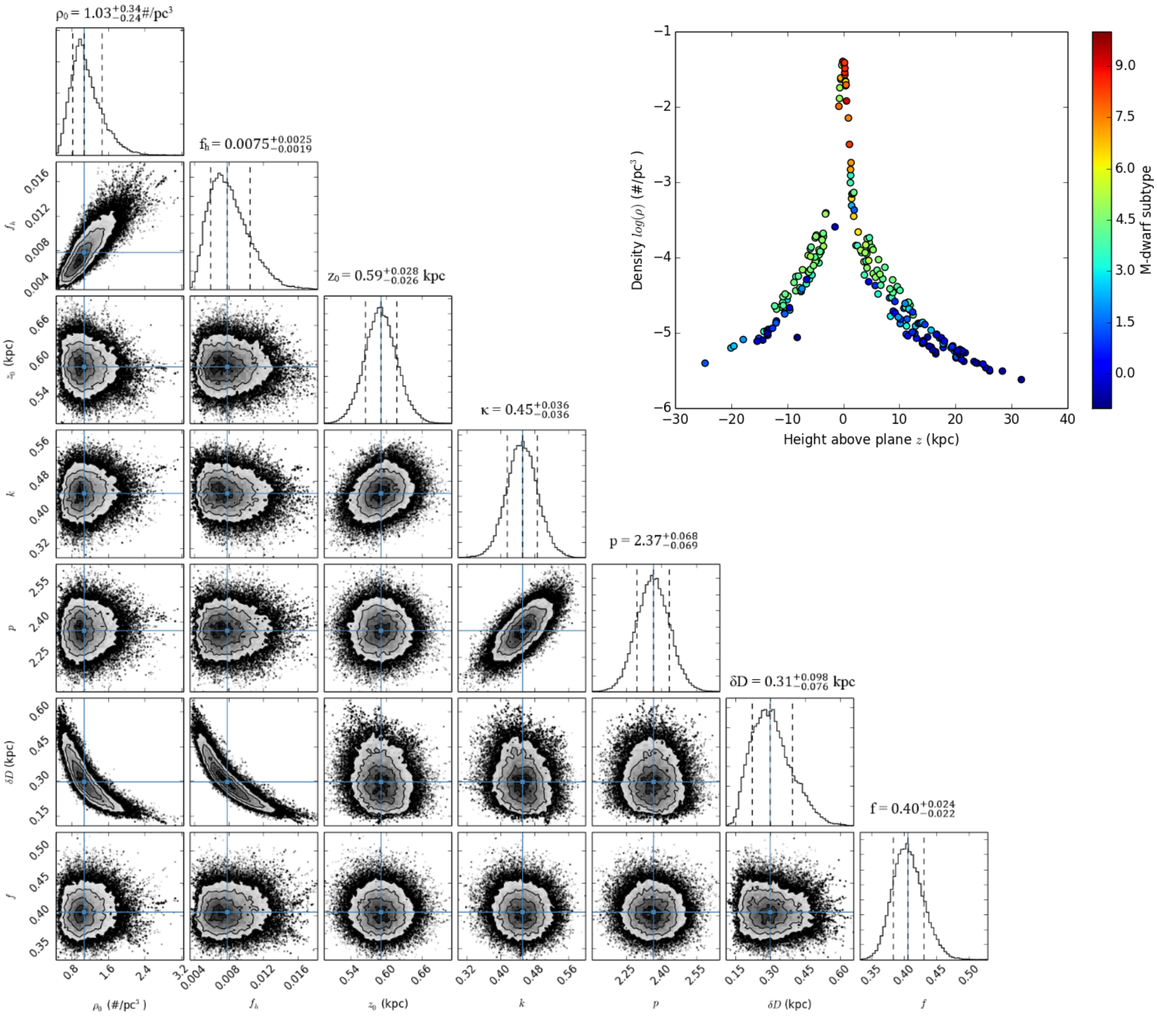

Figure 2 Corner plot of subtypes M0 up to and including M9. The dotted lines give the 16th and 84th percentiles which are used for the uncertainties. The found values are given in the figure. The figure in the right corner is a density plot made with the halo-disk model. On the horizontal axis is shows the height above the plane. We can see that within the disk the distribution of M-dwarfs is denser than that of the halo. The colour bar represents the subtypes of the M-dwarfs. Most of the older and dimmer types are found within the disk instead of the halo, which can be explained by the fact that we are more sensitive to the brighter types in the halo than we are to the dimmer ones.

starting point [13]. The walkers are initialized in a small ball around the optimized values. The boundaries of the priors are set on physically expected values, but are very broad. The results are presented in a corner plot (Figure 2).

This corner plot shows all the one and two dimensional projections of the posterior probability distributions of our parameters. The marginalized distributions for each parameter are presented in the histograms along the diagonal and the marginalized two dimensional distributions are presented in the other panels. The latter quickly demonstrates degeneracies between parameters, which means they are correlated. The two dimensional distributions in the corner plots turn out banana shaped when this is the case. Generally, it is something that one would like to avoid when fitting a model with several parameters. This is because of the fact that for two degenerate parameters different combinations within parameter space can give similar likelihood values.

The uncertainties are based on the 16th and 84th percentiles of the marginalized distributions, which represent a standard deviation of respectively -1σ and 1σ.

The corner plot of the fitted model shows a degeneracy between f_h and δD and between δD and ρ_0 has appeared. κ - p and f_h- ρ_0 show some degeneracy.

Total number

With the found parameters for the halo-disk model, we can compute the number of M-dwarfs in the disk and halo by integrating the model. The number is $26.7^{+9.3}_{-6.2} \times 10^9$.

Fraction

Now that we have the total mass in the halo and disk, we can find the fraction of halo M-dwarfs and compare it with the theoretical model developed by Cooper et al 2013 [14]. This model gives the relation between accreted mass and the total stellar mass. This relation was found from numerical simulations.

The fraction of halo stars we found is 7^{+5}_{-4}%, higher than the 2% fraction found by Courteau et al. 2011 [15]. In

Figure 3 we display the found value for the fraction and the total stellar mass of the Milky Way of Courteau et al. 2011 [15] with the model of Cooper et al 2013 [14]. We see that our value found for the halo fraction of the Milky Way lies within the margins of the model.

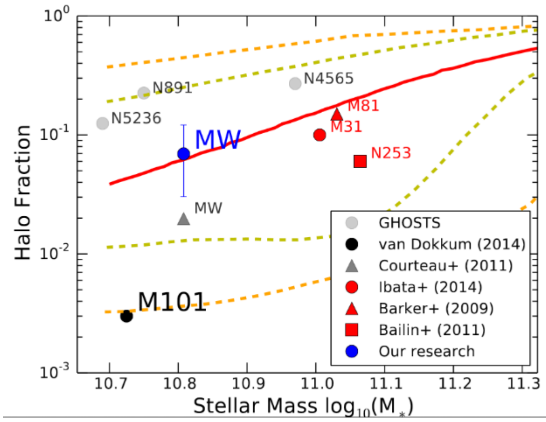

For the calculation of the halo fraction we do not take the bulge and the possible thick disk into account. Provided

Figure 3 The mass fraction in the stellar halo as a function of the total stellar mass. The red line is the predicted median relation between the accreted mass fraction and the total stellar mass [14]. The green and orange line indicate the respectively the 1σ and 2σ limits.

that they contribute considerably, adding them could lead to a lower halo fraction. One that is more in accordance with the value found by Courteau et al. 2011 [15]. We therefore have obtained an upper limit of the halo fraction.

CONCLUSION

We have found that the model that best fits the used data is the halo-disk model. For the scale height z_0 of the the disk we found 0.60±0.03 kpc. The flattening parameter κ and powerlaw-index for the halo p were found to be respectively 0.45±0.04 and 2.4±0.07. The total number of M-dwarfs in the disk and halo was determined to be $26.7^{+9.3}_{-6.2} \times 10^9$, with a total mass upper limit of $1.99^{+0.73}_{-0.5} \times 10^9$ M⊙. The upper limit for the halo fraction of M-dwarfs in the halo 7^{+5}_{-4} %. The estimate for the number of M-dwarfs can be helpful for EUCLID: there will be a notion of how many M-dwarfs can be expected in the survey. EUCLID will be able to detect all M-dwarfs and nearly all streams and satellite galaxies of the Milky Way. With this data the halo substructure can be detected and the density model of the Milky Way can further be improved.

ROLE OF THE STUDENT

Isabel van Vledder and Dieuwertje van der Vlugt were Bachelor students working under the supervision of Dr. Benne Holwerda when the research in this report was performed. The topic was proposed by the supervisor. The design of the questionnaire, the processing of the results as well formulation of the conclusions and the writing were done by the students.

REFERENCES

1. LeBlanc F. 2010. *An introduction to stellar astrophysics.* Wiley, first edition.
2. Wilkins S. M., Stanway E. R., Bremer M. N. 2014. *"High-redshift galaxies and low-mass stars."* MNRAS 439:1038-1050.
3. Scalo J. M. 1986. *"The stellar initial mass function."* Fund. Cosmic Phys. 11:1-278.
4. Holwerda B. W. et al. 2014. *"Milky Way Red Dwarfs in the BoRG Survey; Galactic Scale-height and the Distribution of Dwarf Stars in WFC3 Imaging."* ApJ 788:77.
5. Hawley S. L. et al. 2002. *"Characterization of M, L, and T Dwarfs in the Sloan Digital Sky Survey."*AJ 123:3409-3427.
6. Bovy J., Rix H.-W., Liu C., Hogg D. W., Beers T. C., Lee Y. S. 2012b. *"The Spatial Structure of Mono-abundance Sub-populations of the Milky Way Disk."* ApJ 753:148.
7. Cheng J. Y. et al. 2012. *"A Short Scale Length for the α-enhanced Thick Disk of the Milky Way: Evidence from Low-latitude SEGUE Data."* ApJ 752:51.
8. Bensby T., Alves-Brito A., Oey M. S., Yong D., Meléndez J. 2011. *"A First Constraint on the Thick Disk Scale Length: Differential Radial Abundances in K Giants at Galactocentric Radii 4, 8, and 12 kpc."* ApJ 735:L46.
9. Reid I. N., Cruz K. L., Kirkpatrick J. D., Allen P. R., Mungall F., Liebert J., Lowrance P., Sweet A. 2008. *"Meeting the Cool Neighbors. X. Ultracool Dwarfs from the 2MASS All-Sky Data Release."* AJ 136:1290-1311.
10. Jurić M. et al. 2008. *"The Milky Way Tomography with SDSS. I. Stellar Number Density Distribution.*"ApJ 673:864-914.
11. Foreman-Mackey D., Hogg D. W., Lang D., Goodman J. 2013. *"emcee: The MCMC Hammer."* PASP 125:306-312.
12. Weisz D. R. et al. 2013. *"The Panchromatic Hubble Andromeda Treasury. IV. A Probabilistic Approach to Inferring the High-mass Stellar Initial Mass Function and Other Power-law Functions."* ApJ 762:123.
13. Brooks S., Gelman A., Jones G., Meng X.-L. 2011. *Handbook of Markov Chain Monte Carlo*. CRC press.
14. Cooper A. P., D'Souza R., Kauffmann G., Wang J., Boylan-Kolchin M., Guo Q., Frenk C. S., White S. D. M. 2013. *"Galactic accretion and the outer structure of galaxies in the CDM model."* MNRAS 434:3348-3367.
15. Courteau S., Widrow L. M., McDonald M., Guhathakurta P., Gilbert K. M., Zhu Y., Beaton R. L., Majewski S. R. 2011. *"The Luminosity Profile and Structural Parameters of the Andromeda Galaxy."* ApJ 739:2